

An Astrometric Study of Red Lights in Cambridge

Dominic Ford
Cavendish Laboratory, Madingley Road, Cambridge, CB3 0HE.

November 24, 2005

Contents

1	Introduction	1
2	Experimental Method	2
2.1	Determination of the Bearings of Red Lights from Various Locations	3
2.2	Triangulation of the O.S. Grid References of the Red Lights . . .	3
2.2.1	Finding the Most Likely Position of Sources	3
2.2.2	Finding the Uncertainty in (X_0, Y_0)	4
2.2.3	Finding σ_i	5
3	Results: Measurement of Bearings	6
3.1	Bearing from Wimpole Way (OS 428.2 587.4)	8
3.2	Bearing from Wimpole Way (OS 427.5 587.4)	9
3.3	Bearing from Wimpole Way (OS 427.2 586.2)	10
3.4	Bearing from Castle Mound (OS 445.9 591.9)	11
4	Results: Triangulation of Sources	12
4.1	Source A	12
4.2	Source B	12
4.3	Source C	12
4.4	Source D	12
5	Conclusion	13

1 Introduction

In 2003, whilst walking to Coton, Church & Ford (2003) noted the curious phenomenon of a series of red lights visible on the south-eastern horizon from Wimpole Way, Cambridge. It was first suggested that these sources might be located on the roof of a building to the south of the Cambridge Athletics Ground,



Figure 1: A photograph of a series of red lights which are visible on the southeastern horizon from Castle Mound.

or along Grange Road. However, exhaustive searches of these locations yielded no promising candidates. Later suggestions included one that the lights were located on the Department on Engineering. However, on a subsequent walk to Grantchester, the same authors noted that the sources were also visible from Grantchester Meadows, and, in 2005 May, it was further determined that these sources were visible from Comberton.

Despite Ford's most impassioned pleas with Church that further investigation of the source of these red lights would be an excessively arduous activity for very little gain, Church was insistent that such a study should be carried out. It was proposed that the red lights in question might emanate from Addenbrooke's Hospital. In this paper, an astrometric argument is developed which demonstrates that, beyond all reasonable doubt, this is the origin of one of the said red lights. The remaining lights appear to be associated with a building not marked on the 2001 O.S. map, possibly recently built.

Figure 1 shows a photograph of these sources from Wimpole Way. It is noted that a tight cluster of lights is seen, with three separate lesser lights at some distance to the south. Hereafter, we shall refer to the tight cluster of lights as source A, and the lesser lights, from north to south, as sources B, C and D respectively.

2 Experimental Method

The bearings of the aforementioned red lights were measured from a number of locations around Cambridge, and used to triangulate the position of their source. The method for measuring the bearings at each location is described in section 2.1. Then, in section 2.2, a Bayesian method for combining these bearings to triangulate a probability density function for the positions of the red lights is developed.

2.1 Determination of the Bearings of Red Lights from Various Locations

Night time photographs of the aforementioned red lights were taken on clear nights from a number of locations around Cambridge. Known stars were identified in each image, and their celestial positions found from the *Yale Bright Stars Catalogue*. Using the known time and date of each observation, these were projected onto altitude and azimuth basis vectors. We denote the altitude of each star α , and its azimuth β . Using the measured (x, y) pixel positions of each these stars in each image, a transformation of the form

$$\begin{pmatrix} \alpha \\ \beta \end{pmatrix} = \mathcal{R}(\theta) \left[\begin{pmatrix} m_x & 0 \\ 0 & m_y \end{pmatrix} \begin{pmatrix} x \\ y \end{pmatrix} - \begin{pmatrix} a_x \\ a_y \end{pmatrix} \right], \quad (1)$$

where $\mathcal{R}(\theta)$ is a clockwise rotation matrix:

$$\mathcal{R}(\theta) = \begin{pmatrix} \cos \theta & -\sin \theta \\ \sin \theta & \cos \theta \end{pmatrix},$$

connecting each (x, y) location in each image to its corresponding (α, β) , was fitted for each image by minimising, via the free parameters $\{m, \theta, a_x, a_y\}$, the square residuals in the resultant β values for the known stars. No fit was made to the α values, which are plagued by atmospheric refraction effects close to the horizon. The curvative of the celestial (α, β) coordinate system was neglected in this calculation, though it is noted that all of the following measurements are made near the horizon where the effect is minimal. Optical aberrations in the images were further neglected. However, a more detailed calculation taking both of these effects into account can be found in Church (2005, not yet in prep.).

No error estimate in the calculated values of β are made at this stage; they are made retrospectively by a calculation described in section 2.2.3.

2.2 Triangulation of the O.S. Grid References of the Red Lights

In this section, we develop a Bayesian method for determining the most likely position of each of the red lights from our observed bearings. We assume that for each source we have N observations, made from O.S. grid references $\{x_i, y_i\}$, yielding azimuthal positions β_i . We denote the uncertainty in β_i as σ_i . For the purposes of the present calculation, we assume σ_i to be known; we show how its value may be calculated in section 2.2.3.

In the following section, we find the probability distribution function for the position (X, Y) of each source, denoting its most likely position (X_0, Y_0) .

2.2.1 Finding the Most Likely Position of Sources

We write the probability distribution function for the position (X, Y) of each source as:

$$\begin{aligned}
P &= P(X, Y | \{x_i, y_i, \beta_i, \sigma_i\}, I) \\
&= \frac{P(\{\beta_i\} | \{x_i, y_i, \sigma_i\}, X, Y, I) \times P(X, Y | \{\sigma_i\}, I)}{P(\{\beta_i\} | \{\sigma_i\}, I)},
\end{aligned}$$

where I represents any background knowledge that we have of the problem. Assuming a uniform prior, and neglecting the evidence, which is independent of the values of X and Y , we can write:

$$P \propto \prod_{i=1}^N \frac{1}{\sigma_i \sqrt{2\pi}} \exp\left(\frac{-[\beta_i - \tan 2^{-1}(X - x_i, Y - y_i)]^2}{2\sigma_i^2}\right),$$

where $\tan 2^{-1}()$ is a four-quadrant inverse tangent function. We simplify the mathematics by minimising not P , but its logarithm, L :

$$L = - \sum_{i=1}^N \left(\frac{-[\beta_i - \tan 2^{-1}(X - x_i, Y - y_i)]^2}{2\sigma_i^2} \right).$$

This is minimised numerically over (X, Y) space to yield (X_0, Y_0) . It may be noted that, if the uncertainties σ_i of all of our observations are assumed equal, then the position of this minimum is independent of them.

2.2.2 Finding the Uncertainty in (X_0, Y_0)

We find the uncertainty in the most likely position (X_0, Y_0) of each red light by taking a Taylor expansion of L about (X_0, Y_0) :

$$\begin{aligned}
L(X, Y) &= L(X_0, Y_0) + \underbrace{(X - X_0) \frac{\partial L}{\partial m} \Big|_{X_0, Y_0} + (Y - Y_0) \frac{\partial L}{\partial X} \Big|_{X_0, Y_0}}_{\text{Zero at maximum}} + \dots \\
&\quad \frac{(X - X_0)^2}{2} \frac{\partial^2 L}{\partial m^2} \Big|_{X_0, Y_0} + \frac{(Y - Y_0)^2}{2} \frac{\partial^2 L}{\partial c^2} \Big|_{X_0, Y_0} + \dots \\
&\quad \frac{2(X - X_0)(Y - Y_0)}{2} \frac{\partial^2 L}{\partial Y \partial X} \Big|_{X_0, Y_0} + \mathcal{O}(X - X_0)^3 \dots
\end{aligned}$$

Using Gauss' Method, we identify the above terms containing second derivatives of L as the Gaussian components of P . We write this term, which we denote Q , in matrix form:

$$Q = \frac{1}{2} \begin{pmatrix} X - X_0 & Y - Y_0 \end{pmatrix} \underbrace{\begin{pmatrix} A & B \\ B & C \end{pmatrix}}_{\text{Hessian } \mathbf{A} \equiv \nabla \nabla L} \begin{pmatrix} X - X_0 \\ Y - Y_0 \end{pmatrix}, \quad (2)$$

where:

$$A = \frac{\partial^2 L}{\partial X^2} \Big|_{X_0, Y_0} \quad B = \frac{\partial^2 L}{\partial Y \partial X} \Big|_{X_0, Y_0} \quad C = \frac{\partial^2 L}{\partial Y^2} \Big|_{X_0, Y_0}$$

To determine the probability distribution for X , we marginalise P over Y :

$$P(X | \{x_i, y_i, \beta_i, \sigma_i\}, I) = \int_Y P(X, Y | \{x_i, y_i, \beta_i, \sigma_i\}, I) dY$$

Assuming the probability distribution to be a pure Gaussian, we substitute expression (2) into the above, and complete the square in the exponential term to yield a tractable Gaussian integral:

$$\begin{aligned} &= \exp\left(\frac{1}{2}(X - X_0)^2 \left(A - \frac{B^2}{C}\right)\right) \int_Y \exp\frac{C}{2} \left((Y - Y_0) + \frac{B(X - X_0)}{C}\right)^2 dY \\ &\propto \exp\left(\frac{1}{2}(X - X_0)^2 \left(A - \frac{B^2}{C}\right)\right) \sqrt{\frac{2\pi}{C}} \end{aligned}$$

We conclude by inspection that the standard deviation of X is:

$$\sigma_X = \sqrt{\frac{C}{AC - B^2}}$$

By symmetry, it may also be noted that:

$$\sigma_Y = \sqrt{\frac{A}{AC - B^2}}$$

The algebraic proof of this result, which is trivial, is left as an exercise for the reader.

The values of σ_X and σ_Y depend critically upon the uncertainties σ_i , and so a Bayesian method for estimating these is developed in the following section.

2.2.3 Finding σ_i

We assume that the uncertainties in all of our observations are equal, and therefore that $\sigma_i = \sigma$. We treat the determination of σ as a Bayesian model selection problem, maximising the posterior probability for σ given by:

$$P(\sigma | I) \propto \underbrace{P(\{x_i, y_i, \beta_i\} | \sigma, I)}_{\text{Evidence}} \times \underbrace{P(\sigma)}_{\text{Prior}}.$$

We assume a uniform prior, which makes the task of maximising the above posterior probability equivalent to that of maximising the Bayesian evidence function. This can be written as:

$$P(\{x_i, y_i, \beta_i\} | \sigma, I) = \int_X \int_Y P(\{x_i, y_i, \beta_i\} | X, Y, \sigma, I) P(X, Y | \sigma, I) dX dY.$$

Assuming a uniform prior for (X, Y) , the probability distribution being integrated over XY space above may be expected to exhibit a single Gaussian-like peak centred on (X_0, Y_0) , and the integrals may be approximated by the analytical integral of a Gaussian distribution of the same peak height and width:

$$P(\{x_i, y_i, \beta_i\} | \sigma, I) \simeq \underbrace{P(\{x_i, y_i, \beta_i\} | X_0, Y_0, \sigma, I)}_{\text{Likelihood for best fit case}} \underbrace{P(X_0, Y_0 | \sigma, I) \Delta X \Delta Y}_{\text{Occam Factor}}$$

$\Delta X \Delta Y$ is the area of XY space which is within one standard deviation of the best fit parameters (X_0, Y_0) . In general, the contours of equiprobability will take the form of off-axis ellipses in hypothesis space, and $\Delta X \Delta Y$ is equal to the product of the major and minor axes of the one sigma error ellipse. This does not equal the product of the marginal standard deviations σ_X and σ_Y , except when the x and y axes are aligned with the principal axes of these ellipses. To evaluate $\Delta X \Delta Y$, we return to the Hessian matrix \mathbf{A} defined in expression (2). By a rotation in XY space, we transform into the eigenvector basis of \mathbf{A} , thus diagonalising \mathbf{A} . In this basis, (X', Y') , the errors along the two axes are uncorrelated, and are given by $\sigma_{X'} = \lambda_{X'}^{-1/2}$ and $\sigma_{Y'} = \lambda_{Y'}^{-1/2}$, where λ is used to denote the eigenvalues of \mathbf{A} . Thus, $\Delta X \Delta Y$ is equal to $2\pi \text{Det}^{-1/2}(\mathbf{A})$, where the factor of 2π arises from integration over a two-dimensional Gaussian. However, as determinants are geometrically invariant under rotations, this result is true in all bases:

$$\Delta X \Delta Y = 2\pi \text{Det}^{-1/2}(\mathbf{A}) = \frac{2\pi}{\sqrt{AC - B^2}}$$

As in the previous section, it is easier to maximise the logarithm of the evidence, which we denote L_2 , than the evidence itself:

$$L_2 = - \sum_{i=1}^N \left(\frac{[\beta_i - \tan 2^{-1}(X - x_i, Y - y_i)]^2}{2\sigma^2} - \log_e \left(\frac{1}{\sigma\sqrt{2\pi}} \right) \right) + \log_e \left(\frac{2\pi}{\sqrt{AC - B^2}} \right)$$

This may be maximised numerically, calculating A , B and C numerically by second differencing.

3 Results: Measurement of Bearings

Observations were made from Wimpole Way and from Castle Mound. Ordinance Survey grid references for these locations were determined (see the map fragments shown in figure 2). For each observation, the (x, y) pixel locations of bright stars in the image are listed, along with their right ascensions and declinations, as found in the *Yale Bright Stars Catalogue*, and their altitudes and azimuths, as calculated for the time and date of observation. The best fitting values of $\{m, \theta, a_x, a_y\}$ are listed, followed by the (x, y) pixel locations of each of the sources A, B, C and D. The azimuths (i.e. bearings) are then computed for each source.



Figure 2: Ordnance Survey map fragments of the observing locations. Top map, Wimpole Way, centred on O.S. grid square 42 58. Lower map, Castle Mound, centred on O.S. grid square 44 59.

3.1 Bearing from Wimpole Way (OS 428.2 587.4)

Reproduction of Photograph



Observation Time: 2005 October 29, 21h33 UT

Identification of Bright Stars

Star name	x	y	R.A.	Dec.	Alt.	Az.
π -Ceti	1107	436	2 ^h 44.400 ^m	-13°49.971'	16°12.338'	139°56.237'
ρ -Ceti	1208	301	2 ^h 26.231 ^m	-12°15.792'	19°23.888'	143°33.197'
ρ 3-Eridani	785	306	3 ^h 04.561 ^m	-07°34.606'	19°39.441'	132°22.569'
ϵ -Eridani	573	510	3 ^h 33.204 ^m	-09°26.223'	14°35.750'	126°50.238'
ζ -Eridani	708	404	3 ^h 16.116 ^m	-08°47.803'	17°13.915'	130°19.562'
τ 4-Eridani	931	866	3 ^h 19.777 ^m	-21°44.114'	05°24.605'	135°46.455'
τ 3-Eridani	1104	855	3 ^h 02.650 ^m	-23°36.020'	05°31.808'	140°09.678'
τ 2-Eridani	1148	717	2 ^h 51.304 ^m	-20°58.727'	09°01.134'	141°25.891'
τ 1-Eridani	1154	607	2 ^h 45.376 ^m	-18°32.804'	11°48.558'	141°42.438'

Best Fitting Parameters

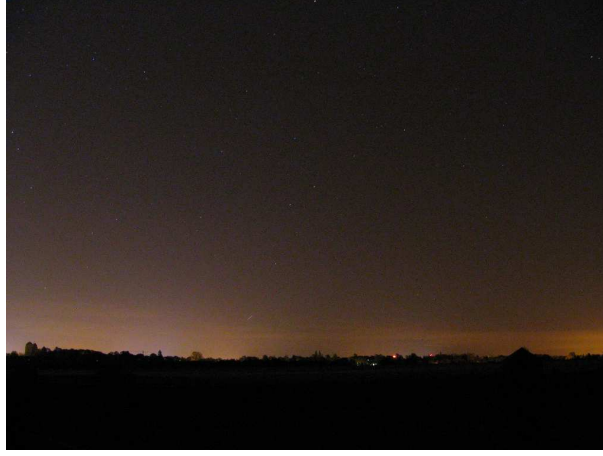
m_x	m_y	θ	a_x	a_y
2.582×10^{-2}	5.660×10^{-3}	96.832°	1.100×10^2	-2.72×10^1

Observed Positions of Sources

Source	x	y	Az.
A	930	1045	135.58°
B	1054	1037	138.76°
C	1058	1036	138.87°
D	1060	1039	138.92°

3.2 Bearing from Wimpole Way (OS 427.5 587.4)

Reproduction of Photograph



Observation Time: 2005 October 29, 21h39 UT

Identification of Bright Stars

Star name	x	y	R.A.	Dec.	Alt.	Az.
π -Ceti	1546	577	2 ^h 44.400 ^m	-13°49.971'	16°48.000'	141°19.801'
ρ -Ceti	1680	440	2 ^h 26.231 ^m	-12°15.792'	19°56.714'	145°00.201'
ρ 3-Eridani	1252	447	3 ^h 04.561 ^m	-07°34.606'	20°20.506'	133°47.232'
ϵ -Eridani	1041	648	3 ^h 33.204 ^m	-09°26.223'	15°20.354'	128°10.074'
ζ -Eridani	1175	545	3 ^h 16.116 ^m	-08°47.803'	17°56.340'	131°41.941'
τ 4-Eridani	1391	1011	3 ^h 19.777 ^m	-21°44.114'	06°03.380'	137°01.229'
τ 3-Eridani	1576	1005	3 ^h 02.650 ^m	-23°36.020'	06°07.345'	141°24.809'
τ 2-Eridani	1615	864	2 ^h 51.304 ^m	-20°58.727'	09°35.686'	142°43.846'
τ 1-Eridani	1622	751	2 ^h 45.376 ^m	-18°32.804'	12°22.882'	143°02.667'

Best Fitting Parameters

m_x	m_y	θ	a_x	a_y
2.588×10^{-2}	-2.221×10^{-2}	87.118°	1.025×10^2	-8.419

Observed Positions of Sources

Source	x	y	Az.
A	1312	1220	134.53
B	1433	1216	137.66
C	1438	1215	137.79
D	1440	1220	137.84

3.3 Bearing from Wimpole Way (OS 427.2 586.2)

Reproduction of Photograph



Observation Time: 2005 October 29, 21h44 UT

Identification of Bright Stars

Star name	x	y	R.A.	Dec.	Alt.	Az.
π -Ceti	1421	601	2 ^h 44.400 ^m	-13°49.971'	17°16.860'	142°29.907'
ρ -Ceti	1559	470	2 ^h 26.231 ^m	-12°15.792'	20°23.139'	146°13.200'
ρ 3-Eridani	1135	460	3 ^h 04.561 ^m	-07°34.606'	20°53.945'	134°58.364'
ϵ -Eridani	916	653	3 ^h 33.204 ^m	-09°26.223'	15°56.854'	129°17.090'
ζ -Eridani	1054	555	3 ^h 16.116 ^m	-08°47.803'	18°30.958'	132°51.126'
τ 4-Eridani	1253	1028	3 ^h 19.777 ^m	-21°44.114'	06°34.963'	138°03.871'
τ 3-Eridani	1429	1027	3 ^h 02.650 ^m	-23°36.020'	06°36.198'	142°27.737'
τ 2-Eridani	1479	889	2 ^h 51.304 ^m	-20°58.727'	10°03.663'	143°49.162'
τ 1-Eridani	1491	777	2 ^h 45.376 ^m	-18°32.804'	12°50.642'	144°09.913'

Best Fitting Parameters

m_x	m_y	θ	a_x	a_y
2.642×10^{-2}	2.383×10^{-3}	98.331°	1.066×10^2	-5.514×10^{-1}

Observed Positions of Sources

Source	x	y	Az.
A	1078	1254	133.28
B	1199	1253	136.44
C	1204	1251	136.57
D	1206	1255	136.62

3.4 Bearing from Castle Mound (OS 445.9 591.9)

Reproduction of Photograph



Observation Time: 2005 November 10, 01h23 UT

Identification of Bright Stars

Star name	x	y	R.A.	Dec.	Alt.	Az.
Adhara	396	713	6 ^h 58.852 ^m	−28°58.676′	03°56.976′	150°06.041′
σ -Canis Majoris	332	664	7 ^h 01.948 ^m	−27°56.466′	04°40.422′	149°05.456′
Wesen	205	603	7 ^h 08.625 ^m	−26°24.024′	05°33.387′	147°08.032′
α 2-Canis Majoris	224	423	7 ^h 03.265 ^m	−23°50.385′	08°23.081′	147°18.467′
α 1-Canis Majoris	359	404	6 ^h 54.372 ^m	−24°11.366′	08°47.087′	149°21.133′
Furud	930	635	6 ^h 20.535 ^m	−30°03.831′	05°30.488′	158°23.221′
ξ 2-Canis Majoris	610	251	6 ^h 35.299 ^m	−22°58.040′	11°22.079′	153°08.492′
ξ 1-Canis Majoris	664	267	6 ^h 32.097 ^m	−23°25.231′	11°09.460′	153°59.767′
γ -Lepus	1340	55	5 ^h 44.705 ^m	−22°26.666′	14°42.812′	164°37.636′
HIP28675	1112	351	6 ^h 03.493 ^m	−26°16.949′	10°05.538′	151°07.697′

Best Fitting Parameters

m_x	m_y	θ	a_x	a_y
1.677×10^{-2}	1.435×10^{-3}	68.927°	1.511×10^2	7.208

Observed Positions of Sources

Source	x	y	Az.
A	778	919	156.19°
B	958	921	159.01°
C	988	918	159.48°
D	997	925	159.62°

4 Results: Triangulation of Sources

4.1 Source A

Best fitting position:

$$(463.6, 551.6)$$

Hessian matrix for this position:

$$Q = \begin{pmatrix} -0.402 & -0.310 \\ -0.310 & -0.272 \end{pmatrix}$$

Axes of one sigma error ellipse are of length 70 m along bearing 140.9°, and of length 12 m along bearing 50.9°.

4.2 Source B

Best fitting position:

$$(462.3, 548.9)$$

Hessian matrix for this position:

$$Q = \begin{pmatrix} -0.332 & -0.233 \\ -0.233 & -0.186 \end{pmatrix}$$

Axes of one sigma error ellipse are of length 82 m along bearing 143.8°, and of length 14 m along bearing 53.8°.

4.3 Source C

Best fitting position:

$$(461.7, 549.4)$$

Hessian matrix for this position:

$$Q = \begin{pmatrix} -0.380 & -0.264 \\ -0.264 & -0.209 \end{pmatrix}$$

Axes of one sigma error ellipse are of length 76 m along bearing 144.0°, and of length 13 m along bearing 54.0°.

4.4 Source D

Best fitting position:

$$(461.6, 549.5)$$

Hessian matrix for this position:

$$Q = \begin{pmatrix} -0.383 & -0.265 \\ -0.265 & -0.210 \end{pmatrix}$$

Axes of one sigma error ellipse are of length 75 m along bearing 144.0°, and of length 13 m along bearing 54.0°.

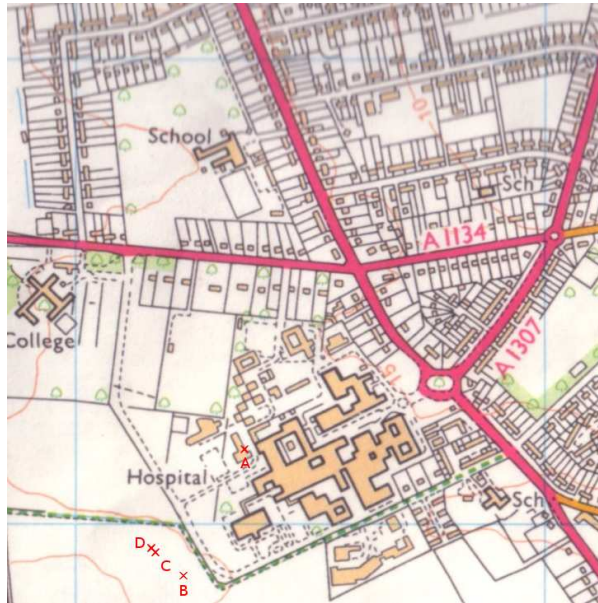


Figure 3: Ordnance Survey map fragment showing the locations of the red lights, labelled A, B, C and D. Map in centred on O.S. grid square 46 55.

5 Conclusion

It has been shown beyond all reasonable doubt that the tight cluster of red lights visible from Wimpole Way, Castle Mound, Grantchester Meadows and Comberton emanate from Addenbrooke's Hospital. It is concluded that the aforementioned hospital has a group of big red lights on top. It is further concluded that there is another unidentified building, to the south-west of the Addenbrooke's site, and not marked on the 2001 O.S. map, which also has big red lights on top. Perhaps Addenbrooke's have recently built an extension.